

Time-resolved Kerr microscopy of coupled transverse domain walls in a pair of curved nanowires

P. S. Keatley, W. Yu, L. O'Brien, D. E. Read, R. P. Cowburn, and R. J. Hicken

Citation: [Journal of Applied Physics](#) **115**, 17D507 (2014); doi: 10.1063/1.4865211

View online: <http://dx.doi.org/10.1063/1.4865211>

View Table of Contents: <http://scitation.aip.org/content/aip/journal/jap/115/17?ver=pdfcov>

Published by the [AIP Publishing](#)

Articles you may be interested in

[Micromagnetic analysis of current-induced domain wall motion in a bilayer nanowire with synthetic antiferromagnetic coupling](#)

[AIP Advances](#) **6**, 056409 (2016); 10.1063/1.4944769

[Application of local transverse fields for domain wall control in ferromagnetic nanowire arrays](#)

[Appl. Phys. Lett.](#) **101**, 192402 (2012); 10.1063/1.4766173

[Current-induced coupled domain wall motions in a two-nanowire system](#)

[Appl. Phys. Lett.](#) **99**, 152501 (2011); 10.1063/1.3650706

[Magnetic imaging of the pinning mechanism of asymmetric transverse domain walls in ferromagnetic nanowires](#)

[Appl. Phys. Lett.](#) **97**, 233102 (2010); 10.1063/1.3523351

[Asymmetric ground state spin configuration of transverse domain wall on symmetrically notched ferromagnetic nanowires](#)

[Appl. Phys. Lett.](#) **97**, 022511 (2010); 10.1063/1.3459965

A promotional banner for AIP Applied Physics Reviews. The background is a dark blue gradient with a bright light source on the right, creating a lens flare effect. On the left, there is a small image of a book cover for 'AIP Applied Physics Reviews' featuring a diagram of a layered structure. The main text 'NEW Special Topic Sections' is in large, white, bold font. Below this, the text 'NOW ONLINE' is in yellow, followed by 'Lithium Niobate Properties and Applications: Reviews of Emerging Trends' in white. The AIP Applied Physics Reviews logo is in the bottom right corner.

NEW Special Topic Sections

NOW ONLINE
Lithium Niobate Properties and Applications:
Reviews of Emerging Trends

AIP Applied Physics
Reviews

Time-resolved Kerr microscopy of coupled transverse domain walls in a pair of curved nanowires

P. S. Keatley,^{1,a)} W. Yu,¹ L. O'Brien,^{2,3} D. E. Read,⁴ R. P. Cowburn,³ and R. J. Hicken¹

¹*School of Physics and Astronomy, University of Exeter, Stocker Road, Exeter EX4 4QL, United Kingdom*

²*Department of Chemical Engineering and Materials Science, University of Minnesota, 421 Washington Ave. SE, Minneapolis, Minnesota 55455, USA*

³*Thin Film Magnetism Group, Cavendish Laboratory, University of Cambridge, JJ Thompson Avenue, Cambridge CB3 0HE, United Kingdom*

⁴*School of Physics and Astronomy, Cardiff University, Queen's Buildings, The Parade, Cardiff CF24 3AA, United Kingdom*

(Presented 6 November 2013; received 23 September 2013; accepted 7 November 2013; published online 21 February 2014)

Time-resolved scanning Kerr microscopy has been used to directly observe magnetostatically coupled transverse domain walls (TDWs) in a pair of closely spaced, curved nanowires (NWs). Kerr images of the precessional response of the magnetic domain to either side of the TDW revealed the TDW as a minimum in the Kerr signal in the region of closest NW separation. When the TDWs were ejected from the NW pair, the minimum in the Kerr signal was no longer observed. By imaging this transition, the static de-coupling field was estimated to be in the range from 38 to 48 Oe in good agreement with a simple micromagnetic model. This work provides a novel technique by which DC and microwave assisted decoupling fields of TDWs may be explored in NW pairs of different width, separation, and curvature. © 2014 AIP Publishing LLC. [<http://dx.doi.org/10.1063/1.4865211>]

The static and dynamic dipolar interactions are perhaps the most obvious mechanisms by which to couple the magnetic behaviour of two individual nanomagnets when their separation is similar to their size. Coupled magnetic systems are interesting from both fundamental and technological perspectives^{1,2} since the static magnetic configurations and associated resonances can be continuously tuned using a magnetic field.³ In contrast to a nanomagnet, the magnetization of a transverse domain wall (TDW) in a planar nanowire (NW) is only confined across the NW width, but free to move along the NW length. Therefore, coupled TDWs are a relatively simple (1D) system in which the static and dynamic dipolar coupling can be studied.^{4,5} In this work, we use time-resolved scanning Kerr microscopy⁶ (TRSKM) to directly observe magnetostatically coupled TDWs and estimate their static de-coupling field. Measurement of the static de-coupling field of coupled TDWs is important for the development of domain wall logic,⁷ and race track memory devices.⁸

Pairs of curved NWs of different width, separation, and radius of curvature were fabricated along the center of a Ti/Au(200 nm) coplanar stripline (CPS) of length $L = 16$ mm with $63 \mu\text{m}$ wide tracks separated by $5 \mu\text{m}$. Electron-beam lithography was used to fabricate the NW pairs from a thermally evaporated $\text{Ni}_{80}\text{Fe}_{20}$ (10 nm) film on a Si substrate. Here, we report measurements on a pair of 300 nm wide NWs with $1.5 \mu\text{m}$ radius of curvature and inner edge-to-edge separation of 30 nm.

TRSKM was used to study the dynamic response of the NW pair, Figure 1(a). A Ti:Sapphire oscillator was used to

generate ~ 100 fs laser pulses with 800 nm wavelength at a repetition rate of 80 MHz. The laser pulses were synchronised with the pulsed output waveform of an impulse generator. The pulsed waveform was amplitude modulated at a frequency of ~ 3.1 kHz before passing through the CPS. The resulting time-varying (and modulated) magnetic field was used to excite magnetization dynamics within the NWs. The out-of-plane component of the dynamic magnetization was detected at normal incidence using the polar Kerr effect. The laser pulses were expanded ($\times 5$), re-collimated, linearly polarized, and then focused to a diffraction limited spot of ~ 500 nm diameter using a $\times 60$ microscope objective. The polar Kerr rotation Φ_K was detected using a polarizing balanced photodiode bridge detector.⁹ A lock-in amplifier was used to recover the modulated Kerr signal at 3.1 kHz. TR traces were acquired by fixing the position of the laser spot on the NW sample and recording the Kerr rotation as a function of time by scanning a 4 ns optical delay. TR images were acquired by fixing the time delay and scanning the sample beneath the laser spot using a piezo-electric stage. A large (~ 2 kOe) in-plane reset magnetic field H_R was applied to the NW sample using a quadrupole electromagnet.

TDWs were formed in the NWs by applying H_R in the y -direction, Figure 1(b).¹⁰ As H_R is reduced to remanence, micromagnetic simulations¹¹ show that the magnetization in each NW relaxes towards opposite x -directions to form two domains with a TDW at the center of each NW. In Figure 1(b), the magnetizations in the domains of the upper NW are tail-to-tail (TT), while those of the lower NW are head-to-head (HH).⁴ Since the TDWs form at the closest point of separation, this will now be referred to as the TDW interaction region. The TDWs can be ejected from the NW pair by applying H_R in the x -direction, Figure 1(c).¹⁰ When the field

^{a)}Author to whom correspondence should be addressed. Electronic mail: p.s.keatley@exeter.ac.uk.

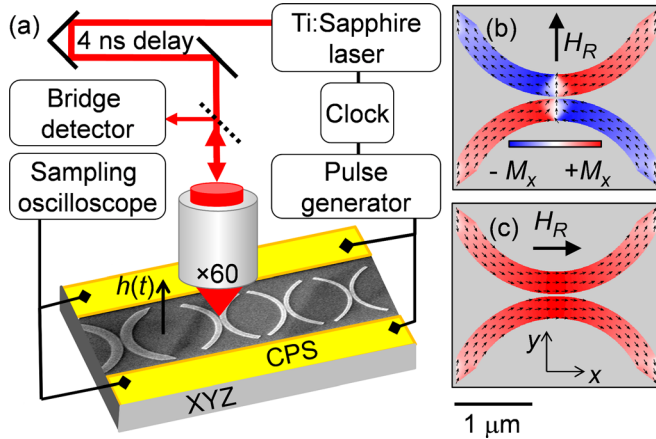


FIG. 1. (a) A schematic of the experimental geometry with an out-of-plane pulsed magnetic field excitation $h(t)$. Part of the NW sample is shown in the SEM image inset between the CPS tracks. The simulated equilibrium states of a NW pair are shown for perpendicular (b) and parallel (c) reset fields H_R . The red and blue color scales represent $+M_x$ and $-M_x$, respectively.

is reduced to remanence, the magnetization relaxes to form a single domain, where the magnetization follows the curvature of the NWs. TR images acquired at a maximum of the polar Kerr precession signal are shown for the NW pair with and without TDWs in Figures 2(a) and 2(b), respectively. It was not possible to couple to the TDW resonance¹² using an out-of-plane pulsed magnetic field. However, by imaging the precessional response within the domains, the TDWs can be detected. The Kerr image in Figure 2(a) reveals a small reduction of the Kerr signal in the interaction region, while in Figure 2(b), the Kerr signal appears to be more uniform, and perhaps slightly enhanced in the interaction region. The enhanced signal is due to the magneto-optical contribution from both NWs in the interaction region.¹² This effect also occurs when the TDWs are present in the NWs, and leads to a smaller reduction in the Kerr signal than might be expected from micromagnetic simulations (inset). The difference in

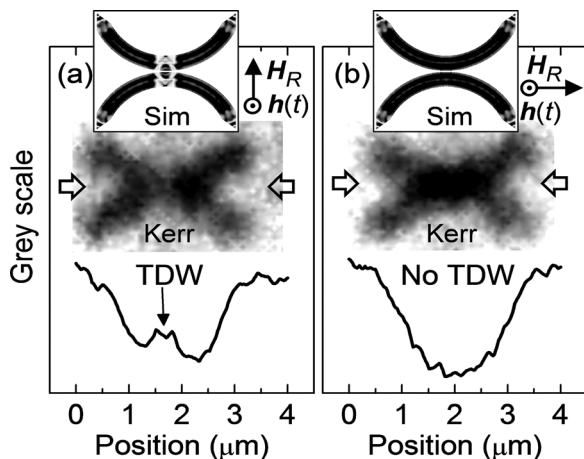


FIG. 2. TR Kerr images for the NW pair (a) with and (b) without TDWs. Contrast profiles, shown below the Kerr images, are plotted on the same grey scale in (a) and (b). The profiles were extracted from a $4 \times 0.25 \mu\text{m}^2$ region that was taken horizontally through the center of the interaction region (width and position indicated by block arrows). Corresponding simulated images of the out-of-plane component of the dynamic magnetization are inset in (a) and (b).

Kerr signal is clearly seen in horizontal contrast profiles extracted from a 250 nm wide section taken through the center of the interaction region. In Figure 2(a), the contrast profile shows a clear reduction in the black contrast at the expected location of the TDWs (indicated by arrow), while no such reduction is observed in Figure 2(b) indicating the absence of the TDWs. The inset simulated images of the out-of-plane component of the dynamic magnetization show that the TDWs lead to a complicated response that cannot be spatially resolved experimentally. In the interaction region, the precession frequency will vary due to the continuously changing magnetization and internal field resulting in a net reduction in the out-of-plane component of the dynamic magnetization, as observed experimentally in the Kerr images.

When TDWs are present in the interaction region, a stray magnetic field is generated by uncompensated magnetic dipoles at the inner edges of the NWs. Since the HH and TT TDWs have opposite net magnetostatic charge, the magnetic potential is attractive, and the TDWs are magnetostatically coupled.⁴ Here, we estimate the static de-coupling field of the TDWs using TRSKM. Figure 3(a) shows TR signals acquired from the interaction region of the NW pair shown in Figures 2(a) and 2(b). A TR signal acquired from the left-most end of the upper NW in Figure 2(a) shows that the precession has similar phase near to the ends of the NW, while the amplitude is slightly reduced, since only a single NW is probed. When TDWs are present (absent) in the interaction region, the precession frequency was 3.8 GHz (3.56 GHz). The higher frequency, when TDWs are present, is consistent with an increase in the demagnetizing field since the magnetization is confined across the width of the NW. In addition, the static dipolar field of one TDW may contribute to the total internal field within the other TDW. When the TDWs are ejected, the magnetization is parallel to the length of the NW so the demagnetizing and stray field contributions to the internal field are reduced.

In Figure 3(b), a sequence of TR Kerr images is shown. The images were acquired at time delay τ in Figure 3(a) for which the precession signals with and without TDWs show

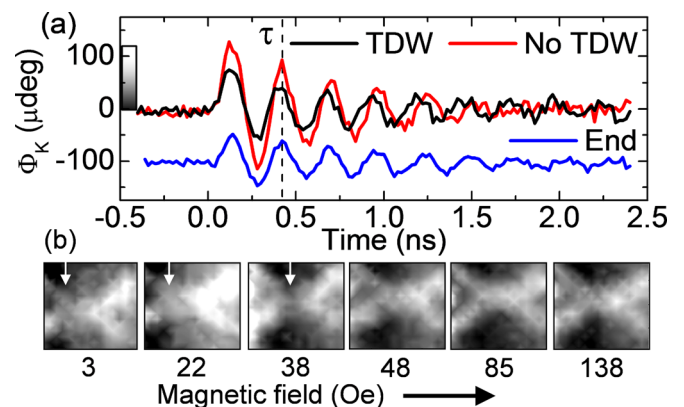


FIG. 3. (a) TR Kerr signals acquired at remanence from the interaction region with (black curve) and without (red curve) TDWs, and from the end of a NW (blue curve, offset for clarity). (b) A sequence of TR Kerr images acquired at remanence and at delay τ after a magnetic field of increasing amplitude has been applied in the x -direction.

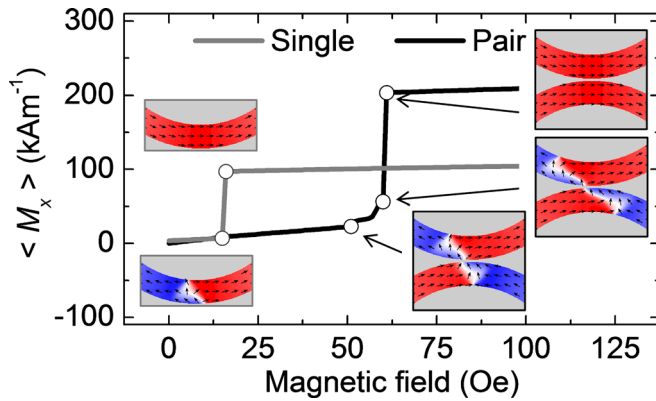


FIG. 4. Simulated magnetization curves for single and pair NW configurations. Inset maps of the static magnetization are shown, where red and blue indicate $+M_x$ and $-M_x$, respectively. The height of the curve for the NW pair is twice that of the single NW since only one NW is present in the simulated mesh in the latter case.

temporal overlap so that it is possible to observe the transition between NWs with and without TDWs. First TDWs were generated in the interaction region (with pulse generator switched off). H_R was reduced to remanence and the orientation rotated 90° . The first image in Figure 3(b) shows the dynamic response at remanence (~ 3 Oe). A reduction in Kerr signal observed slightly to the left of the interaction region (indicated by arrow) indicates the presence of the TDWs. The shift of this region may be due to pinning of the TDWs at edge defects to the left of the interaction region.

Before each image, a magnetic field was applied, while the impulse generator was switched off to avoid resonance assisted de-coupling of the TDWs. The field strength was increased between subsequent images, but then reduced to remanence for the acquisition of each image. Images acquired after applying a field of 22 Oe and 38 Oe, still show the reduced region of Kerr intensity to the left of the interaction region. Differences in the first three images may be attributed different pinning sites of the TDWs after larger magnetic fields have been applied.

Images acquired after a field of 48 Oe was applied, show the TR Kerr signal to be more uniform throughout the NW pair, with little difference observed after 85 Oe, 138 Oe, and $H_R \sim 2$ kOe (not shown) was applied, indicating that after 48 Oe, the TDWs were ejected. Therefore, the static TDW de-coupling field is estimated to be between 38 Oe and 48 Oe.

To understand if the experimental TDW de-coupling field was reasonable, magnetization curves (starting from zero field) were simulated for single and pair NW configurations and assume no edge roughness or thermal effects. Figure 4 shows the averaged M_x component of the static magnetization averaged over the simulated mesh. For the single NW, the TDW was ejected at 15 Oe. In contrast, the TDWs of the NW pair were ejected via a series of metastable states. Initially, the TDWs are displaced as the domains with magnetization parallel to the applied field

grow at the expense of the antiparallel domains. The TDWs are displaced in opposite directions owing to the TT and a HH domain structure. Up to 51 Oe, the TDWs retain their remanent state structure. However, as the field is increased to 60 Oe, the TDWs are stretched, but remain coupled at the point of closest separation. Above 60 Oe, the TDWs are decoupled, ejected, and the magnetization in each NW forms a single domain. Experimentally, it is unlikely that the metastable states at larger values of the applied field will be realized due to thermal activation of the switching process. The experimental estimate of the TDW de-coupling field was found to be between $\sim 60\%$ and 80% of the zero temperature simulated values, in agreement with previous reports.¹³

In summary, we have used TRSKM to directly observe the presence of TDWs in a pair of curved NWs with HH and TT domain structure. From TR Kerr images, the value of the static de-coupling field was estimated to be 38 to 48 Oe in good agreement with a simple micromagnetic model and previous reports. While TRSKM was used to characterise the static de-coupling field in this work, dynamic coupling and microwave assisted de-coupling may be explored by using an in-plane RF magnetic field to couple to the NW resonances.¹² This experimental approach may prove to be a powerful tool for the characterisation of interacting TDWs.

This work was supported by the EU Grant Master No. NMP-FP7-212257, the UK EPSRC Grant Ref. EP/I038470/1, and partially supported by the EU FP7 Project 3SPIN No. 247368, and the Marie Curie IOF Project No. 299376.

¹V. V. Kruglyak, S. O. Demokritov, and D. Grundler, *J. Phys. D: Appl. Phys.* **43**, 264001 (2010).

²S. O. Demokritov and A. Slavin, *Magnonics: From Fundamentals to Applications* (Springer, Heidelberg, 2013).

³B. Pigeau, C. Hahn, G. de Loubens, V. V. Naletov, O. Klein, K. Mitsuzuka, D. Lacour, M. Hehn, S. Andrieu, and F. Montaigne, *Phys. Rev. Lett.* **109**, 247602 (2012).

⁴L. O'Brien, E. R. Lewis, A. Fernández-Pacheco, D. Petit, R. P. Cowburn, J. Sampaio, and D. E. Read, *Phys. Rev. Lett.* **108**, 187202 (2012).

⁵I. Purnama, M. C. Sekhar, S. Goolaup, and W. S. Lew, *Appl. Phys. Lett.* **99**, 152501 (2011).

⁶P. S. Keatley, P. Gangmei, M. Dvornik, R. J. Hicken, J. Grollier, C. Ulysse, J. R. Childress, and J. A. Katine, in *Magnonics*, edited by S. O. Demokritov and A. N. Slavin (Springer, Berlin, Heidelberg, 2013), Vol. 125, p. 17.

⁷D. A. Allwood, G. Xiong, C. C. Faulkner, D. Atkinson, D. Petit, and R. P. Cowburn, *Science* **309**, 1688 (2005).

⁸S. S. P. Parkin, M. Hayashi, and L. Thomas, *Science* **320**, 190 (2008).

⁹Since the full beam was sampled on each photodiode, there was no sensitivity to the in-plane component of the dynamic magnetization via the longitudinal Kerr effect.

¹⁰E. Saitoh, H. Miyajima, T. Yamaoka, and G. Tatara, *Nature* **432**, 203 (2004).

¹¹See supplementary material at <http://dx.doi.org/10.1063/1.4865211> for details of the micromagnetic simulations.

¹²A. T. Galkiewicz, L. O'Brien, P. S. Keatley, R. P. Cowburn, and P. A. Crowell, "Resonance in Magneto-statically Coupled Transverse Domain Walls," e-print [arXiv:1402.3202](https://arxiv.org/abs/1402.3202).

¹³L. O'Brien, D. Petit, H. T. Zeng, E. R. Lewis, J. Sampaio, A. V. Jausovec, D. E. Read, and R. P. Cowburn, *Phys. Rev. Lett.* **103**, 077206 (2009).